Theoretical and Applied Climatology (2022) 150:955–968
https://doi.org/10.1007/s00704-022-04213-2

ORIGINAL PAPER

Statistical characteristics of sea-effect snow events over the western Black Sea

Veli Yavuz[1,2] · Anthony R. Lupo[2] · Neil I. Fox[2] · Ali Deniz[1,3]

Received: 1 March 2022 / Accepted: 14 September 2022 / Published online: 17 September 2022

Abstract

In this study, the structural classification of sea-effect snow (SES) events occurring over the western Black Sea was made for the period between 2009 and 2018. The main purpose of this study is to determine the meso- and synoptic-scale structures of SES events for the region and to form the basis for nowcasting and forecasting applications. Aviation reports published by four airports in the Marmara Region were analysed, and snowy periods were found. Then, SES bands detected by visual evaluation of satellite and radar images were followed temporally and spatially. Finally, SES events were classified by considering the inland extensions of SES bands along their trajectories, the snowfall conditions in the regions where they pass, and the meso- and synoptic-scale systems affecting snowfall. A total of 95 events were identified. Of these events, 36 were determined as Black Sea (BS) events (38%), 24 were Synoptic-scale (SYNOP) events (25%), 23 were Over Sea Convergence (OSC) events (24%) and 12 were Transition (TRANS) events (13%). The mean duration of the SES events was 15.9 h. The longest event occurred in the SYNOP-Events type and lasted 59 h. It was found that SYNOP-Events lasted longer on average than others. The prevailing wind direction was northerly (NW, N, NE), except for OSC-Events. An inversion layer was detected in most of the BS-Events and SYNOP-Events, and average temperature differences between the sea surface (SS) and the upper level air (850/700 hPa) were approximately 4 °C to 6 °C above the threshold values presented in similar studies in the literature. In the annual statistical analysis, the greatest number of the events was 20 in 2016, no events occurred in 2009 and only two events occurred in 2012. No trend was found on an annual basis. On a monthly basis, the greates number of the events occurred in January (51), while the least events occurred in March (2).

1 Introduction

Lake-effect snow (LES) occurs as a result of a cold air parcel passing over a relatively warmer water body (lake), transferring heat (sensible and latent) and moisture fluxes from its body, and reaching saturation (Niziol et al. 1995; Kristovich et al. 2003). A similar mechanism applies to sea-effect snow (SES). For the analyses performed in this study, the expression "SES" was preferred instead of "LES". The parameters mentioned in this definition have important meteorological and physical effects in the occurrence of LES/SES events. These parameters are detailed as follows: the origin, moisture content and trajectory of the cold air mass; topographic structure and size of the water body over which the cold air passes; surface temperature of this water body; presence of an upper level mechanism that limits the vertical development of convection; wind speed/direction conditions on the water surface and upper atmospheric levels; wind shears between surface and upper atmospheric levels (850-, 700-hPa levels). In studies examining the effect of meteorological variables on LES/SES events, many case studies have been carried out for the Baltic Sea (Pike and Webb 2020) and Black Sea (Yavuz et al. 2021a). In addition, climatological analyses were performed for the Black Sea (Yavuz et al. 2021b), Lake Michigan (Kelly 1982), Lake Erie (Wiley and Mercer 2020), Lake Ontario (Hartnett et al. 2014; Wiley and Mercer 2020), Lake Tahoe (Laird et al. 2016) and Pyramid Lake (Laird et al. 2016).

In the studies conducted in the twentieth century, LES events have been subjected to various classifications by

✉ Veli Yavuz
yavuzv@itu.edu.tr; veliyavuz@missouri.edu

1 Faculty of Aeronautics and Astronautics, Department of Meteorological Engineering, Istanbul Technical University, ITU Maslak Campus, Maslak, 34469 Istanbul, Turkey

2 Atmospheric Science Program, University of Missouri, 302 E ABNR, Columbia, MO 65211, USA

3 Eurasia Institute of Earth Sciences, Istanbul Technical University, ITU Maslak Campus, Maslak, 34469 Istanbul, Turkey

considering the morphological features of the LES bands and the structural characteristics of the LES events, as well as the determination of the atmospheric conditions in which they occur (Passarelli and Braham 1981; Kelly 1982; Braham 1983; Forbes and Merritt 1984; Niziol et al. 1995). In the twenty-first century, a different classification has been put forward by examining the structural characteristics of the LES events. Laird et al. (2009a) identified 67 LES events that occurred between 1997 and 2006 for Lake Champlain. Afterwards, the structural characteristics of these events were examined in three categories. These categories are as follows: (a) LC-Events (well-defined precipitation occurring independently of synoptic/large-scale systems), (b) SYNOP-Events (semi-stationary precipitation bands embedded within the synoptic-scale system), (c) TRANS-Events (transition between two types). Later, Laird et al (2009b) identified 125 LES events for the New York State Finger Lakes, extending the three categories in the previous study to four categories. Unlike the previous study, Laird et al. (2009b) named the precipitation bands formed as a result of convergence on the lake as "Over Lake Convergence—OLC-Events". A very little or none of these precipitation bands, called the OLC, reach the shore. Finally, Laird et al. (2016) identified 62 LES events over 14 winters for Lake Tahoe and Pyramid Lake. They classified these events in four different categories determined before, according to their structural characteristics. Alcott et al. (2012) used a similar classification to classify LES events according to their structural characteristics.

In the classifications made according to the morphological structures of the LES bands and the structural characteristics of the LES events in the following years, some similar situations are handled with different names. For instance, LC-Events and SYNOP-Events in the classification derived by Laird et al. (2016) are similar in structure to the Type-1,2,3 events classified by Niziol et al. (1995). Also, OLC-Events reflect the Type-5 event. In the literature review, a similar classification proposed by Niziol et al. (1995) was made for the western Black Sea by Yavuz et al. (2021b). However, no study could be found in which the classification of the SES events in the Black Sea according to their structural characteristics [similar classification to Laird et al. (2016)]. In general, the case studies were made in the SES studies for the Black Sea (Kindap 2010; Yavuz et al. 2021a), and climatological analysis of synoptic conditions was performed using the Lamb Weather Type method (Baltaci et al. 2021).

SES occurring in the Marmara Region has negative effects especially on land, air and sea transportations. These effects are shaped by the meso- and synoptic-scale structure of the system. For instance, on 30–31 January 2012, when SYNOP-Events were effective over the Region, a total of 102 flights were cancelled at an international airport in the region. Sea transportation has been temporarily suspended. Dozens of roads were closed to transportation as a result of heavy snow accumulation (Yavuz et al. 2021a). In many events where Black Sea events (BS-Events) were observed, it was stated that the negativities affecting daily life were much more limited compared to Synoptic-scale events (SYNOP-Events) (Yavuz et al. 2022a). The main purpose of this study is to determine the meso- and synoptic-scale structures of SES events for the region and to form the basis for nowcasting and forecasting applications. Accordingly, first, the SES bands that occurred over the western Black Sea between 2009 and 2018 were analysed by using various satellite and radar products. Over a 10-year period, 95 SES events were identified and these events were classified according to their structural characteristics. After classifying events similar to those found in Laird et al. (2016), the atmospheric conditions in which the SES events occurred were analysed for each type. The data used in the study, the detection of the SES bands, and the classification method are defined in Section 2. Statistical results on classification types and atmospheric conditions (meso and synoptic scales) in which these types occur are given in Section 3. Finally, some prominent results were compared with similar studies made for different lakes and seas, and their similarities/differences are revealed in Section 4.

2 Data and methodology

The study period was chosen as 10 years between 2009 and 2018. Snow events were determined by using aviation reports at four airports located in the Marmara Region during this period. Then, the availability of the SES events was investigated by using satellite and radar data for all snow events. Accordingly, no SES band could be detected in 2009. In 2014, only two SES events were detected. Although the determination of snow events from airport reports can be made much more than a 10-year period, satellite and radar images are needed to determine whether these snow events are SES events and to classify them. Difficulties in accessing satellite and radar data (especially radar products) and some airport reports were influential in the classification of the study period as 10 years. In addition, the fact that there are too many types of data sets in the study (for example, four images of two different satellites at 15-min intervals and two images of radar at 7-min intervals were examined for all snow events) required a heavy workload.

2.1 Study region

The Black Sea is bordered by Bulgaria and Romania to the west, Ukraine to the north, Russia and Georgia to the east and Turkey to the south. Besides being a closed sea, it is also connected to the Marmara and Azov Seas. There is the western Black Sea in the north of the Marmara Region and the Marmara Sea in the south. The region, which has a strait connecting the Black Sea to the Marmara Sea, is home to Turkey's metropolitan city, Istanbul, and its strait connects the continents of Asia and Europe. The surface area of the Marmara Region is approximately 67,000 km^2, and the area of the Black Sea is approximately 461,000 km^2 (Demirarslan and Akinci 2018). Especially in the winter season, most precipitation systems enter the region from the north. Therefore, the moisture transfer provided by the western Black Sea to the incoming systems plays an important role in the distribution of precipitation amounts and frequencies. Information about the Black Sea, Marmara Region, radiosonde station and the four airports in the Marmara Region is given in Fig. 1 and Table 1.

2.2 Satellite and radar data

All of the satellite products were obtained for the snow events determined within the period. On the other hand, radar products were only available for the years 2014–2018. In the literature, satellite and radar images have been used in most of the studies on detecting SES bands, classifying them according to their formations and determining their trajectories (Forbes and Merritt 1984; Kelly 1982, 1986; Niziol 1987; Niziol et al. 1995; Yavuz et al. 2021a, 2022a). In this study, the presence, type and trajectory of SES bands at frequent intervals were tried to be understood by analysing various images of both satellite and radar data. The first satellite product used in the study is high-resolution (0.25°×0.25° latitude–longitude resolution) images of the Moderate Resolution Imaging Spectroradiometer (MODIS) module of Terra satellite. The MODIS module, which has 36 spectral bands in 0.4–14.4 µm band range (Zhao and Duan 2020), generates images for the western Black Sea once a day. The images of the MODIS module were accessed from the National Aeronautics and Space Administration (NASA 2021). The second satellite product used in the study is the satellite images in different channels obtained from the Spinning Enhanced Visible and Infrared Imager (SEVIRI) radiometer of the second-generation MSG-2 (Meteosat-9) and MSG-3 (Meteosat-10) satellites of the Meteosat satellite series. The SEVIRI radiometer produces images in four visible (VIS) and near-infrared (NIR) channels in the 0.4–1.6 µm band range, as well as eight

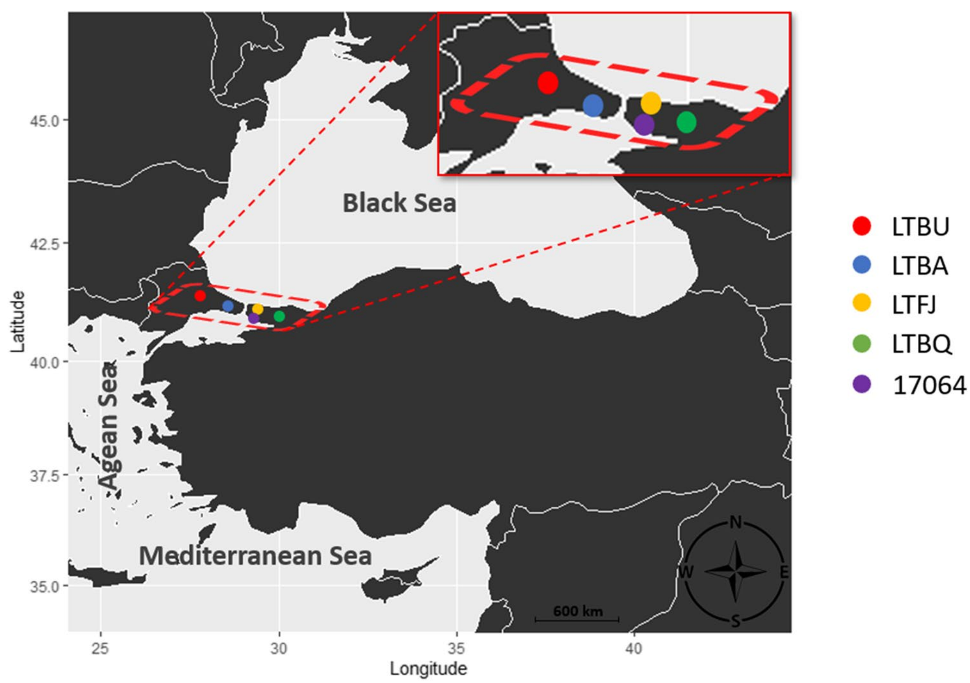

Fig. 1 Locations of the airports and the radiosonde station in the Marmara Region. *LTBU*: Tekirdag Corlu Airport; *LTBA*: Istanbul Ataturk International Airport; *LTFJ*: Istanbul Sabiha Gokcen International Airport; *LTBQ*: Kocaeli Cengiz Topel Airport; *17,064*: Istanbul Kartal Radiosonde Station

Table 1 Information about the airports and the radiosonde station

	Station identifier	Latitude	Longitude	Elevation
Ataturk Int. Airport	LTBA	40°58′34" N	28°48′50" E	50 m
Sabiha Gokcen Int. Airport	LTFJ	40°53′39" N	29°18′30" E	95 m
Kocaeli Cengiz Topel Airport	LTBQ	40°44′10″N	30°5′0″E	55 m
Tekirdag Corlu Airport	LTBU	41°07′46" N	27°54′23" E	16 m
Istanbul Kartal Radiosonde Station	17064	40°54′41"N	29°09′21"E	20 m

infrared (IR) channels in the 3.9–13.4 µm band range (Trigo et al. 2011; Lazri et al. 2020). In this study, infrared band (Channel-9), visible band (Channel-321) and airmass satellite images were analysed. All satellite images were obtained from the Turkish State Meteorological Service (TSMS 2021). Radar images used in the study are images of single polarized C-Band radar located in Istanbul-Catalca district. The Plan Position Indicator (PPI) and Max Display (MAX) images of the radar were analysed. The PPI product is a product related to the location and severity of the system. It scans 360° horizontally with a fixed elevation angle. During this scan, electromagnetic waves are sent to the atmosphere, and the signals (echo) received back from scattered objects in the atmosphere are measured. This product does not detect masses below and above the scanning area. For this reason, the MAX product, which uses a volumetric data set, has been examined for more detailed information about the state of the atmosphere. The MAX product is the product in which the maximum values measured by the radar between two horizontal levels are seen using the volumetric scan data (TSMS 2021). Radar images were obtained from the Turkish State Meteorological Service (TSMS 2021).

2.3 Aviation reports and sounding data

In the study, the Meteorological Aerodrome Reports (METARs) and the Meteorological Aerodrome Special Reports (SPECIs) were obtained for four airports within the borders of the Marmara Region. The reason for choosing these airports is that they represent the majority of the Marmara Region from west to east, and they are the closest airports that meet the systems coming from the Black Sea. The reports were obtained from the IOWA Environmental Mesonet website of IOWA State University (IOWA 2021). Almost all of the aviation reports (97% to 99%) were published within the period. Information on the airports for which METAR and SPECI reports were obtained for the years 2009–2018 is given in Table 1. Three of the four airports (LTBA, LTFJ and LTBU) are in international and one airport (LTBQ) in the national airport categories. While the METAR reports are prepared at half-hourly intervals at international airports in accordance with regional agreements, these reports are mostly prepared hourly at national airports. The SPECI reports are prepared in the event of a meteorological phenomenon that adversely affects aviation activities between two METAR reports. METAR reports, on the other hand, are prepared in the event of a meteorological event that adversely affects aviation activities (events that reduce the visibility, presence of turbulence and strong wind/wind movements, icing) between two meta reports. These meteorological phenomena are usually heavy rainfalls/snowfalls, turbulence, strong/cross winds, icing and fog. The most important reason for using aviation reports in the study is data quality and regular preparation of data at frequent intervals. In the study, actual temperature (T), dew point temperature (Td), relative humidity (RH) and wind speed (Ws) information were provided from these reports and used in the analyses.

In order to provide information about the general vertical structure of the atmosphere, inversion information and wind conditions, the sounding data of Istanbul Kartal Radiosonde Station were provided for 0000 UTC and 1200 UTC for whole period. The data were obtained from the University of Wyoming Atmospheric Sciences website (University of Wyoming 2021).

2.4 Atmospheric vertical level data

Apart from the sounding data, synoptic charts of the 850 hPa and the upper atmospheric levels (700, 500 and 300 hPa) were analysed in order to determine the air movements and to understand the synoptic-scale structure. Air advections, fronts, low/high pressure regions, divergence/convergence areas and temperature/humidity gradients were analysed on 850 hPa charts. The positions, types and trajectories of long- and short-waves over the study area were determined by these constant pressure level maps provided at 6-h intervals. The 500 hPa level has been taken as a reference in many studies in examining the effects of long-waves and associated short-wave troughs on SES events at the synoptic-scale (Tuttle and Davis 2013; Metz et al. 2019; Yavuz et al. 2022b). In this study, in addition to these levels, maps of 700 and 300 hPa levels were also examined in order to understand the vertical development of the existing structure along the vertical atmospheric column. Moreover, surface synoptic charts were analysed to examine the structure and position of the frontal systems, low/high pressure centres and trough/ridge regions. All synoptic charts were obtained from the Plymouth State Weather Center website (PSWC 2021).

2.5 SST data

In the study, the National Oceanic and Atmospheric Administration High-Resolution Blended Analysis (NOAA OI SST V2 High Resolution) dataset was used for the western Black Sea surface temperature information. The dataset was obtained from the Asia–Pacific Data-Research Center website (APDRC 2021). The data represent daily mean values with a latitude–longitude resolution of 0.25° × 0.25° (APDRC 2021). Within the scope of the study, the coordinate "29.50°E, 42.50°N" was preferred for the western Black Sea temperature data. The reason for this is that this point has been seen to show nearly an average value for the western Black Sea region (Yavuz et al. 2021a).

2.6 Detection of the SES bands

First of all, the aviation reports provided for the four selected airports were examined and snow events were determined throughout the entire period. Then, since radar images could not be obtained between 2009 and 2013, images in various bands obtained from devices belonging to the Terra and the MSG satellites were subjected to visual evaluation. For the years 2014–2018, both the mentioned satellite and radar products were subjected to visual evaluation together. In this visual evaluation, each SES class introduced by Laird et al. (2009a, 2009b, 2016) and Alcott et al. (2012) was taken into account. Thus, all SES bands that occurred over the western Black Sea region within the 10-year period have been examined regardless of whether it caused snowfall or not within the boundaries of the Marmara Region.

2.7 SES Event classification

The classification introduced by Laird et al. (2009a, 2009b, 2016) and Alcott et al. (2012) (discussed in the Section 1) was taken as reference in the determination of the SES events. Visual analyses were made by considering the following conditions while classifying through satellite and radar images. First, the areas where the SES bands appear were determined, then the temporal and spatial analyses of the inland extensions along their trajectories were made. Then, the current precipitation conditions were determined by analysing the aviation reports both before and after the SES bands reached the study area. Thus, it was understood whether SES events are pure or not. Finally, the existence and effects of synoptic-scale structures were revealed by analysing the surface and upper level synoptic charts for each event from the moment the SES bands first appeared to the moment they passed into the disintegration stage. After this preliminary evaluation process, the SES events for the western Black Sea were divided into four types:

1. BS-Events (Black Sea Events): These are well-defined events independent of any synoptic-large-scale system over the western Black Sea, with a generally widening structure from north to south, often occurring in more than one parallel band, parallel to flows from the north.
2. OSC-Events (Over Sea Convergence): These are the events that usually occur in the middle parts of the western Black Sea, have little or no extension to the northern flows and usually do not cause any snowfall in the borders of the Marmara Region.
3. SYNOP-Events: They are events that occur with a synoptic and large-scale system (embedded within the system) or immediately after the transition of these systems, having the same morphological structure as the BS-Events, but containing stronger and denser bands. They occur under the influence of frontal systems (especially a cold front), low–high pressure centres (especially the low pressure centre and a cold front associated with it) and trough/ridge structure (mostly the part of the trough that represents the flows descending from the north) observed in the surface synoptic charts. In addition, the OSC-Events embedded in a synoptic/large-scale system and occurring immediately after their passages were transferred to the SYNOP-Events category.
4. TRANS-Events (Transition Events): They are events that show the transition between different types (e.g. BS-Events—SYNOP Events, BS-Events—OSC Events).

In Fig. 2, three different satellite images of the visual evaluation made in determining the Events are given. In the image of BS-Event, parallel band structures reaching the Marmara Region over the western Black Sea are seen in the approximately north/northeast-south/southwest direction. In the image of OSC-Event, band structures observed in different directions and in fragments on the western Black Sea, with a very slight extension to the Marmara Region are seen. In the image of SYNOP-Event, the structure consisting of many bands extending in the northeast-southwest direction, parallel to each other and reaching the Marmara Region is seen. The surface chart (the top left of the bottom figure) shows a low pressure centre located approximately in the south of the eastern Black Sea Region and an occluded front associated with it. It is seen that the front passes over the western Black Sea and the flows are in the same parallel with the bands in the satellite image.

In the study, statistical significance levels of the surface and upper-air meteorological variables were examined for each SES class. First, meteorological parameters were subjected to the normality test (Kolmogorov–Smirnov Test). Then, independent two-sample t test was applied for the parameters that fit the normal distribution. The analysis results of the t tests performed separately for each airport and SES class are given in Table 2.

3 Results

3.1 Frequency, duration and classification of the SES events

As a result of the analysis of the METAR and SPECI reports of four airports between 2009 and 2018, it was found that it was snowy for 186 days. These days were examined using satellite and radar products, and the times of the SES band formation over the western Black Sea were identified. As a result, a total of 95 SES events were determined. The information

Fig. 2 Examples of **a** BS-Event, **b** OSC-Event, **c** SYNOP-Event occurring on the western Black Sea

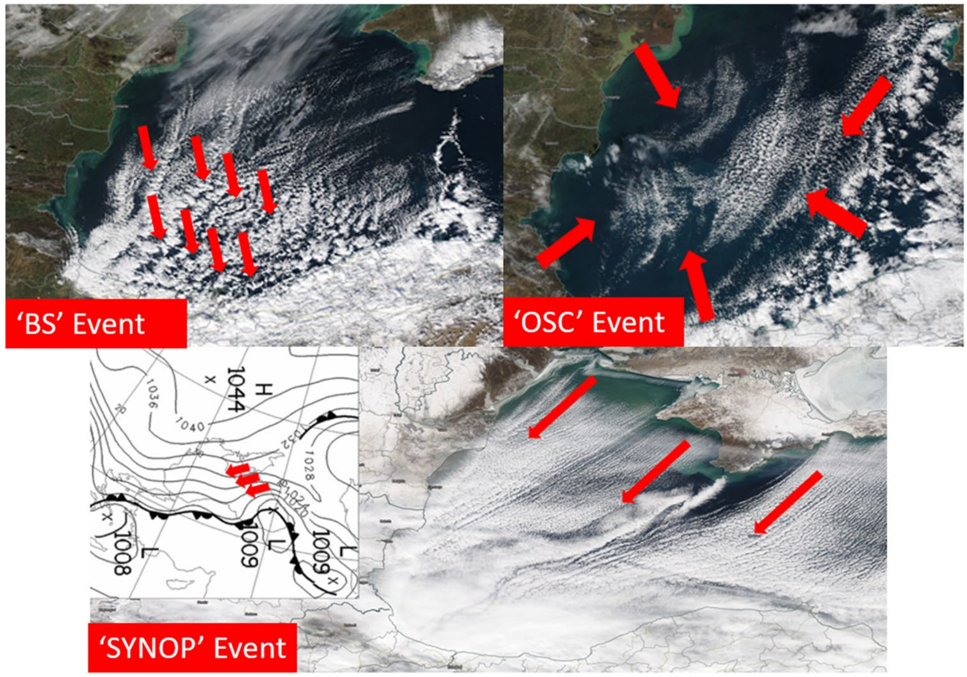

Table 2 The degrees of statistical significance of the data sets analysed in the study for each SES class

Parameter		Statistical significance difference (meaning)			
		BS&SYNOP	*BS&TRANS*	*SYNOP&TRANS*	N-size
LTBA	T (°C)	Not significant	Statistically significant	Statistically significant	BS = 534
	Td (°C)	Statistically significant	Statistically significant	Statistically significant	SYNOP = 782
	RH (%)	Statistically significant	Statistically significant	Statistically significant	OSC = 392
	Ws (kt)	Statistically significant	Not significant	Not significant	TRANS = 32
LFTJ	T (°C)	Not significant	Statistically significant	Statistically significant	BS = 662
	Td (°C)	Statistically significant	Statistically significant	Statistically significant	SYNOP = 902
	RH (%)	Statistically significant	Statistically significant	Statistically significant	OSC = 392
	Ws (kt)	Statistically significant	Not significant	Not significant	TRANS = 36
LTBQ	T (°C)	Not significant	Statistically significant	Statistically significant	BS = 394
	Td (°C)	Statistically significant	Statistically significant	Statistically significant	SYNOP = 515
	RH (%)	Statistically significant	Statistically significant	Statistically significant	OSC = 392
	Ws (kt)	Not significant	Not significant	Not significant	TRANS = 30
LTBU	T (°C)	Not significant	Statistically significant	Statistically significant	BS = 292
	Td (°C)	Statistically significant	Statistically significant	Statistically significant	SYNOP = 334
	RH (%)	Statistically significant	Statistically significant	Statistically significant	OSC = 392
	Ws (kt)	Statistically significant	Not significant	Not significant	TRANS = 38
Over sea	ΔT850-SS(°C)	Statistically significant	Statistically significant	Statistically significant	186
	ΔT700-SS(°C)	Statistically significant	Statistically significant	Statistically significant	186

on how long each event lasted is given in Fig. 3. The mean duration of the SES events was found to be 15.9 h. The longest SES event lasted 59 h. 38% of the events lasted 10 h or less, 68% of them lasted 20 h or less and 86% of them lasted 30 h or less. Three events lasted more than 50 h. In studies for the Great Lakes, the average LES event duration was 12.1 h for the Lake Champlain (Laird et al. 2009a), 9.4 h for the New York State Finger Lakes (Laird et al. 2009b), 7.3 h for the Lake Tahoe (Laird et al. 2016) and 5.6 h for the Pyramid Lake (Laird et al. 2016). Alcott et al. (2012) studied 149 LES events for the Great Salt Lake and found the average event duration to be 11.3 h, also found that the events that occurred in the autumn and winter seasons lasted an average of 3.1 h more than those in the spring seasons. Steenburgh et al. (2000)

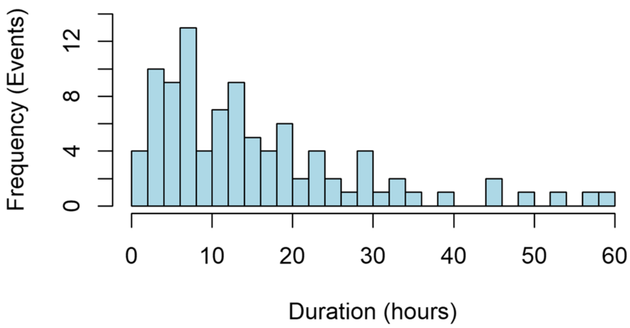

Fig. 3 Duration of the SES events

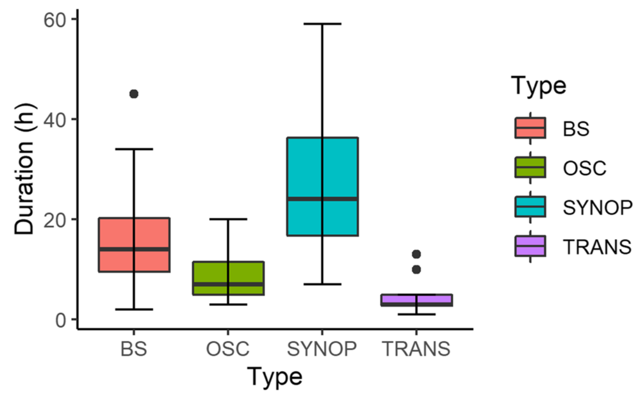

Fig. 4 Box plots showing distribution of duration (h) for **a** BS-Events, **b** OSC-Events, **c** SYNOP-Events and **d** TRANS-Events

stated that the LES event duration for the Great Salt Lake is often greater than 13 h, while for the Great Lake this time can be from 12 h to several days. It has been stated that this difference in event durations in different lakes and in the western Black Sea is related to the size of the water body and the fetch distance (Laird et al. 2016). It has been determined that the western Black Sea has a fetch distance of approximately 600 km (Kindap 2010). The long fetch distance contributes positively to the occurrence of LES/SES events in terms of duration and severity (Laird and Kristovich 2004; Smith and Boris 2017). The main reason for this is that the amount of sensible and latent heat fluxes that the cold air mass will add to its body during its travel over the warmer water masses will be high (Ellis and Leathers 1996; Scott and Sousounis 2001).

The durations of the events for the four types identified based on the structural classification of the SES events were also analysed. Accordingly, the most lasting type on average was SYNOP-Events (27.8 h), followed by BS-Events (16.4 h), OSC-Events (8.5 h) and TRANS-Events (4.5 h). The longest lasting event type was SYNOP-Event (59 h) (Fig. 4). In similar studies in the literature, the average longest event was mostly found as TRANS-Events. For TRANS-Events, Laird et al. (2009a) found this time as 16.6 h and Laird et al. (2009b) as 16.9 h. The most important reason why TRANS-Events had the longest duration was that after the events started as SYNOP-Events, they turned into LC/FL events that were not embedded in the synoptic scale (Laird et al. 2009a, 2009b). In this study, the main reason for the short duration of TRANS-Events was the requirement that the transitions between two different types in TRANS-Events continue uninterruptedly in the transitioned type. In this case, the transition period was determined as a maximum of 6 h without interruption (classification has been carried out in whichever type the switch is made after 6 h), and in interrupted cases (switching to the old type or another type within 6 h), the TRANS-Events category was continued until the uninterrupted condition was met again.

Annual and monthly frequency analyses of each type of the SES events are given in Fig. 5 and Fig. 6, respectively. Each year consists of its own months (Jan, Feb, Mar and Dec). The greatest number of SES events occurred in 2016 (20 events) and at least in 2014 (2 events). No SES event occurred in 2009. No significant trend was detected within the period. Except for the years 2009 and 2014, at least three different types have been observed each year. On a monthly basis, the greatest number of events (51 events) occurred in January, followed by February (24 events), December (18 events) and March (2 events). In other months, a SES event was not observed within the period. Except for the years 2009 and 2014, at least three events (average 7 events) occurred each year in January. Laird et al. (2009a) determined that the highest number of the LES events on a monthly basis were December, February and January, respectively. Laird et al. (2016) found that the most LES events occurred in October for the Lake Tahoe and the Pyramid Lake, respectively. It was also determined that at least 50% of the total LES events occurred in October and November. The main reason for this is that October events mostly occur in the last week of October (Laird et al. 2016), and the temperature differences between the air and the lake surface reach their maximum values during the end of

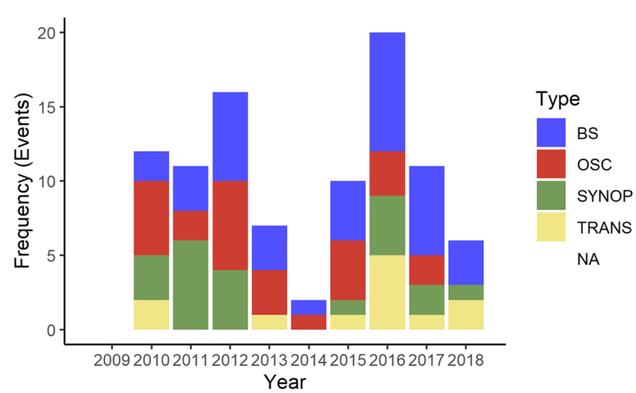

Fig. 5 Annual number of each type of the SES events

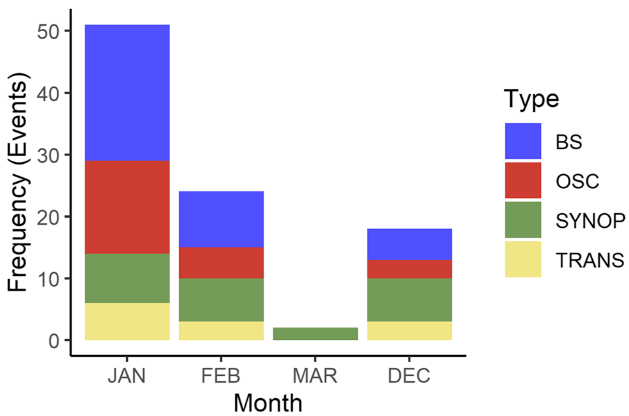

Fig. 6 Monthly number of each type of the SES events

October and November (Alcott et al. 2012). In this study, the number of events observed on a monthly basis and the temperature difference between sea surface (SS) and upper level air temperature (SS-850 hPa; SS-700 hPa) do not show one-to-one proportion. However, the highest average differences were observed in December and January, while February and March had relatively lower averages. It is a normal situation that there is no one-to-one overlap since the analysis was based on the dates of occurrence of SES events only. Considering the difference between SS and upper level air temperature on an average monthly basis for all years, it is thought that results close to those found in the literature, or one-to-one results, will be obtained.

3.2 Factors affecting the occurrence of SES Events

3.2.1 Surface conditions

An analysis was made using surface meteorological information from four airports for the times when the SES Events occurred. For each type of the SES events, analyses were performed for meteorological parameters obtained from the METAR and SPECI reports published by each airport. These meteorological parameters were T, Td, RH and Ws. In the first analysis made, for each SES event, the analysis was made for the meteorological parameters measured during the event periods, regardless of whether there is precipitation at the airports or not.

In the analyses for actual temperature (T), the average values at four airports in BS-Events varied between – 1.6 °C (LTBU) and 1.7 °C (LTBA). Temperature averages in OSC-Events were higher at all airports than in BS-Events. The highest and lowest averages occurred at LTBA (1.8 °C) and LTBU (– 0.6 °C), respectively, similar to those in BS-Events. The lowest actual temperature values in SES types were observed at LTBU. In addition, the fact that it is farther from the Marmara Sea in its south compared to other airports causes terrestrial conditions to be more effective than others. This is due to the fact that the airport is located in the north compared to the other. While lower averages were observed mostly (except LTBQ) in SYNOP-Events, higher values were observed in TRANS-Events (Fig. 7).

In the analyses for dew point temperature (Td), the average values at four airports in BS-Events varied between – 4.2 °C (LTBU) and – 0.7 °C (LTBQ). Lowest and highest dew point temperature averages in OSC-Events occurred at airports similar to those at BS-Events. While higher average values were observed in SYNOP-Events compared to BS-Events (the opposite of the actual temperature), similarly, TRANS-Events had higher values after SYNOP-Events (Fig. 8).

In the analyses for relative humidity (RH), the highest average values were observed in SYNOP-Events (between 74.6 and 93.9%) and BS-Events (between 73.4 and 92.1%) at almost all airports. The highest values among all events were observed at LTBQ (between 88.3 and 93.9%). It has been determined that relative humidity values in SYNOP-Events occurred in a narrower range compared to other events (Fig. 9).

In the analyses for wind speed (kt), the highest average values were observed in SYNOP-Events at all airports. The lowest average values were found in OSC-Events. While the average wind speeds at all airports were 10 kt and above, this value was found to be 3.5 kt at LTBQ (Fig. 10).

In the above analyses, meteorological parameter analyses for all SES events were carried out regardless of whether there was precipitation at the airports. Therefore, for each SES event, analyses of meteorological parameters at the airports during precipitation were also carried out. In this direction, first, the following results were obtained regarding the snowfall conditions at the airports:

- LTBA: Snowfall occurred in 24 (67%) of 36 BS-Events and 20 (83%) of the 24 SYNOP-Events. While there was no snowfall in OSC-Events, snowfall occurred in 1 (8%) of 12 TRANS-Events.
- LTFJ: Snowfall occurred in 31 (86%) of 36 BS-Events and 22 (92%) of the 24 SYNOP-Events. While there was no snowfall in OSC-Events, snowfall occurred in 1 (8%) of 12 TRANS-Events.
- LTBQ: Snowfall occurred in 31 (86%) of 36 BS-Events and 22 (92%) of the 24 SYNOP-Events. While there was no snowfall in OSC-Events, snowfall occurred in 6 (50%) of 12 TRANS-Events.
- LTBU: Snowfall occurred in 17 (47%) of 36 BS-Events and 14 (58%) of the 24 SYNOP-Events. While there was no snowfall in OSC-Events, snowfall occurred in 1 (8%) of 12 TRANS-Events.

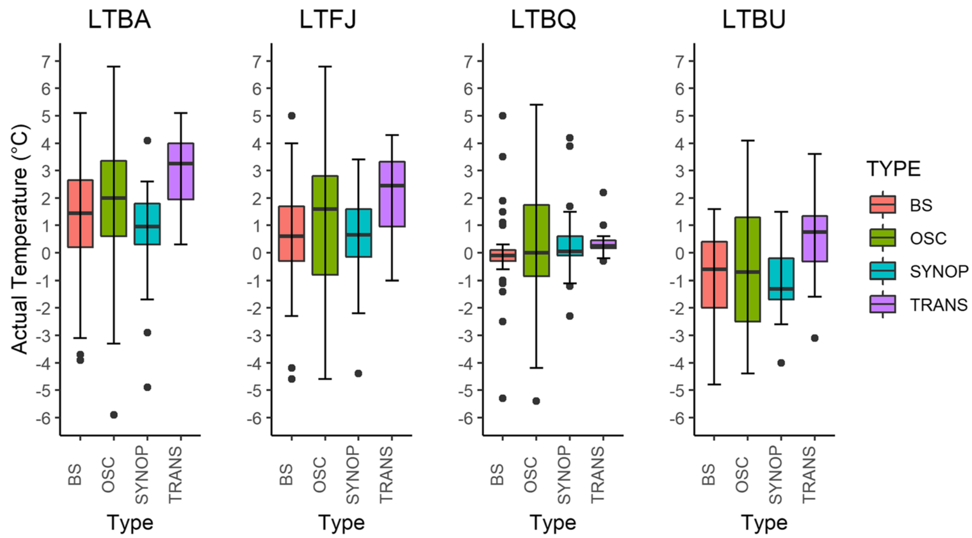

Fig. 7 Box plot of actual temperature (°C) at four airports for each type of the SES events

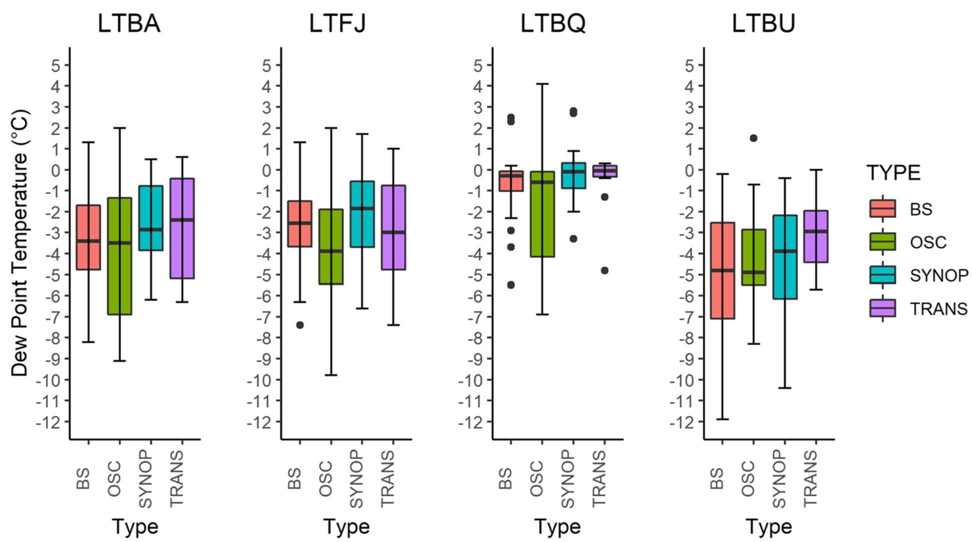

Fig. 8 Box plot of dew point temperature (°C) at four airports for each type of the SES events

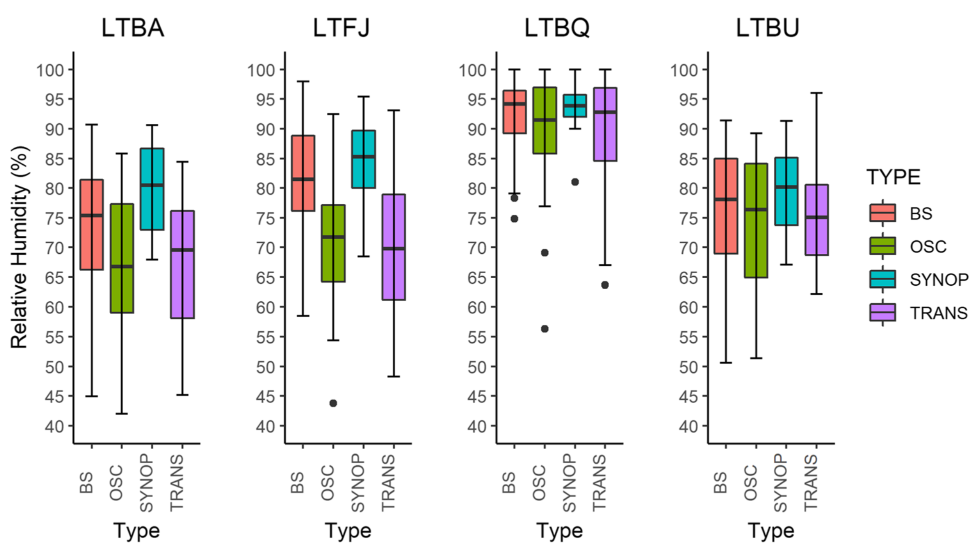

Fig. 9 Box plot of relative humidity (%) at four airports for each type of the SES events

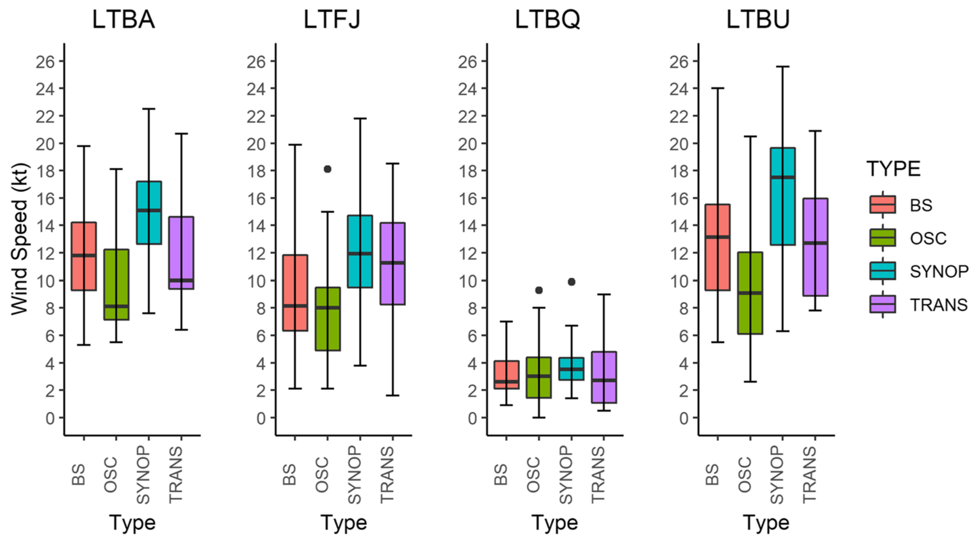

Fig. 10 Box plot of wind speed (kt) at four airports for each type of SES the events

In the light of this information, the average meteorological parameters' analyses at each airport both in snowy times and in the whole period independent of snow are given in Table 3. Analyses were only made for BS-Events and SYNOP-Events, since there was no snowfall at the airports in OSC-Events and TRANS-Events were not evaluated because of the low number. The actual temperature value was found to be lower than the average of the whole period during snowy times at all airports. A similar situation was not observed at the dew point temperature values. Relative humidity values were also observed to be higher mostly in snowy times than the whole period, and a trend was not observed in wind speed values.

In the LES studies conducted for the Lake Champlain and the Finger Lakes, surface average actual air temperatures were – 9 °C and – 8 °C, respectively (Laird et al. 2009a, 2009b). This value was found to be 5.7 °C on average for the Lake Tahoe and the Pyramid Lakes (Laird et al. 2016). Surface average dew point temperatures were – 20 °C for the Lake Champlain (Laird et al. 2009a), – 11 °C for the Finger Lakes (Laird et al. 2009b), – 8.5 °C for the Lake Tahoe (Laird et al. 2016) and – 11 °C for the Pyramid Lakes (Laird et al. 2016). In a study conducted for the Great Lakes Region, it was determined that the Lake Effect Rain event occurs when the surface temperature is greater than 0 °C (Miner and Fritsch 1997). Laird et al. (2009a) determined that SYNOP-Events occur at higher temperatures on average than other events. At the same time, the temperature change range was wider in LC-Events than in SYNOP-Events. In this study, in the analyses made regardless of the snowfall situation for the whole period, the surface actual temperature values were above 0 °C on average at some airports, while it was almost 0 °C or below when snowfall was observed at the airports. Similar to the finding by Laird et al. (2009a), SYNOP-Events occurred at lower temperatures on average and narrower temperature ranges. The main reason for this is that SYNOP-Events occur before the polar or arctic air mass reaches the western Black Sea. The reason for the higher average temperatures at LTBA and LTBU in Istanbul compared to other airports is due to their proximity to the Marmara Sea, which is located in the south, and their location further south. In this study, the average relative humidity values for the snowy period and for the whole period were higher in SYNOP-Events than in BS-Events at all airports. A similar situation was also observed for the average wind speed values. Similar results were also found by Laird et al. (2009a) and Alcott et al. (2012).

Table 3 Average values of T, Td, RH and Ws for BS-Events and SYNOP-Event during snowy times at airports and all times

		Whole Period		Snowy Period	
	Airport	BS	SYNOP	BS	SYNOP
T (°C)	LTBA	1.2	0.7	0.2	0.2
	LTFJ	0.5	0.4	0.1	0.0
	LTBQ	0	0.4	-0.6	-0.3
	LTBU	-1.6	-1.9	-1.3	-2.7
Td (°C)	LTBA	-3.3	-2.6	-2.7	-2.3
	LTFJ	-2.5	-2.1	-1.7	-1.1
	LTBQ	-0.7	-0.2	-1.3	-0.9
	LTBU	-4.2	-4.3	-3.8	-5.0
R (%)	LTBA	73.4	80	82.3	86.0
	LTFJ	81.2	84.6	85.1	88.0
	LTBQ	92.1	93.9	94.2	95.5
	LTBU	76.5	79.3	83.5	84.5
Ws (kt)	LTBA	11.9	15.2	12.9	16.7
	LTFJ	9.2	12.3	9.2	12.5
	LTBQ	3.2	3.8	2.4	3.3
	LTBU	12.7	16.2	15.3	18.3

3.2.2 Sea-atmosphere temperature difference

The temperature difference between SS and 850-hPa level occurred above 17 °C on average for all event types. In the literature, the 13 °C threshold value was used for this difference for the formation of LES events (Rothrock 1969; Holroyd 1971; Niziol 1987; Ballentine 1992; Villani et al. 2017). In this study, it was determined that this difference was around 13 °C in only five of the 95 events, and mostly higher differences occurred. The average temperature difference in BS-Events was higher than the others. Average temperature differences between SS and 700 hPa level were found above 23 °C. This value is well above the 17 °C threshold set forth in the literature (Niziol 1987; Ballentine 1992; Steenburgh et al. 2000; Alcott et al. 2012). Similar to the previous situation, BS-Events had higher differences than the others in almost all averages (Table 4). Sensible and latent heat fluxes moving from the SS to the atmosphere will cause degradation in the lower atmospheric layer, cloudiness and associated precipitation (Ellis and Leathers 1996). The amount of perturbation occurring here will also increase depending on the temperature difference between the SS and the upper atmosphere, and low level atmospheric instability will occur (Scott and Sousounis 2001).

3.2.3 Inversion layer

One of the most important parameters in the occurrence of the LES/SES events is the necessity of a mechanism that will restrict the convectional movement occurring over water bodies at upper atmospheric levels. In this context, it has been suggested that an inversion or capping stable layer should exist (Reinking et al. 1993; Kristovich and Laird 1998). This layer will contribute to the formation of cloudiness and precipitation by limiting perturbation and destabilization due to the transfer of heat and moisture fluxes in the lower atmosphere. While the formation of these layers between 850–700 and 700–500 hPa levels has been put forward as the ideal situation, their occurrence between the surface and the first 150 hPa from the surface has been presented as a negative situation since it will limit the convective movement at very low heights (Steenburgh et al. 2000). In this study, for the specified events, the sounding data published within the period were analysed, and it was revealed whether there was an inversion for each event. The presence of inversion in this observation was given proportionally by examining how many sounding observations there were within the period covered for each event. Among all events, the highest rate of inversion was observed between 850 and 700 hPa, and the lowest rate was between surface and 850 hPa levels (Table 5).

3.2.4 Wind shear

The directional change (Backing/Veering-Cyclonic/Anticyclonic) and the amount of this change (wind shear) of the wind that will occur between the surface/near-surface and the upper atmospheric levels (850 and 700 hPa) are some of the most important parameters affecting the structure, occurrence and stability of the LES/SES bands. For this reason, the fact that the directional change of the wind is less than 30° between the surface and the 850 hPa level (Suriano and Leathers 2017), and less than 60° between the surface and the 700 hPa level (Niziol 1987), provides ideal and strong LES/SES band organizations. In this study, these criteria for BS-Events, SYNOP-Events and TRANS-Events were mostly met, but these criteria could not be met in OSC-Events that could not reach the shore due to the wind direction change over the sea (Table 6). Since there is no supporting synoptic-scale system in BS-Events, it is more important that the amount of wind shear is less in terms of band formation. In SYNOP-Events, on the other hand, the bands were able to maintain their formation in a few cases where the amount of wind shear was slightly above 60°, thanks to the synoptic-scale system. The main reason for this is that the synoptic-scale system affects the characteristics of these bands both in terms of the direction of the flow and due to the high heat and moisture fluxes it incorporates.

Table 5 The frequency of inversions between 1000 hPa and upper atmospheric levels

	Surface—850 hPa	850–700 hPa	700–500 hPa
BS	14%	63%	44%
OSC	24%	67%	55%
SYNOP	20%	48%	40%
TRANS	25%	75%	46%

Table 4 The temperature difference between SS and upper-level air

	Avg. Temp. Diff. (°C)		Max. Temp. Diff. (°C)		Min. Temp. Diff. (°C)	
	SS—850 hPa	SS—700 hPa	SS—850 hPa	SS—700 hPa	SS—850 hPa	SS—700 hPa
BS	18	24.6	22.8	32.4	13.2	15.6
OSC	17.1	23.2	20.5	31	11.8	16.9
SYNOP	17.6	25	21.1	30.1	12.7	15.1
TRANS	17.2	23.6	20.1	30.5	11.2	18

4 Discussion and conclusions

In previous studies, Baltaci et al. (2021) analysed SES events for the Black Sea using a synoptic climatological approach and emphasized the dominance of northern flows. Yavuz et al. (2021b) classified the SES bands according to their morphological structures and examined the effects over the Marmara Region. Depending on the northern flows, the dominance of Type-2 (multi parallel) band (86%) came to the fore. Yavuz et al. (2021a) examined the Type-5 (mesoscale vortex) structure occurring in the western Black Sea and revealed the importance of SS fluxes and wind direction changes for convectional movements and especially for low-level convergence. This study is the first to reveal the structural characteristics of SES events for the western Black Sea region. In this context, classification methods similar to the studies made by Laird et al. (2009a, 2009b, 2016) and Alcott et al. (2012) were used, but significant variations were found in the results. In this study, the mean event duration occurred as 15.9 h. The closest long duration to this is 12.1 h for Lake Champlain calculated by Laird et al. (2009a). It has been shown that the size and fetch distance of the lakes are directly proportional to the average event durations (Laird et al. 2016; Smith and Boris 2017). For the Black Sea, which has a fetch distance of approximately 600 km in the north–south direction and is much larger than these lakes, it is normal for the duration times to be high. Unlike similar studies, the most observed SES event for the western Black Sea was SYNOP-Events. This was followed by BS-Events and OSC-Events. In studies by Laird et al. (2009a, 2009b, 2016), SYNOP-Events were mostly in second place. The result of this study is that the western Black Sea (region) is more exposed to synoptic-scale systems, especially in the transition route of northwest-southwest systems. During the SES times, the frontal systems mostly coming from the northern directions, the fronts connected to the low pressure centres over the eastern Black Sea, and the surface level troughs are the mechanisms that make up the SYNOP-Events.

The two most important parameters for SES events are the temperature difference between SS and the upper level air, and a mechanism that will limit the convectional movement that will occur due to this difference above. With regard to the temperature difference, mostly (95%) the 13 °C threshold (between SS-850 hPa), and the 17 °C threshold (between SS-700 hPa) were exceeded. On average, these values were 17 °C and 23 °C, respectively. Therefore, it has been determined that most of the time, fluxes (heat and moisture fluxes) from the SS to the upper atmosphere cause lower atmospheric destabilization. It is also known that perturbation and lower atmospheric instability will increase depending on the increase in temperature differences (Scott and Sousounis 2001). It is very important to restrict this lower level convectional movement and instability occurring at higher levels. The presence of an inversion layer is important for cloudiness and precipitation, especially the presence after the first 150 hPa from the surface (below it would be an early limitation) (Steenburgh et al. 2000). In this study, low rates of inversion were generally observed in BS-Events and SYNOP-Events (14–20%) at the lower level, while this rate was considerably higher in the middle and upper levels (48–63%).

One of the most important results of the study is that more than half of all events occurred in January. The reason for this is that cold air masses descending from the north pass over the Black Sea more frequently, and meanwhile, sea surface temperatures have positive anomaly values. Another important result of the study is the changes observed in the temperature, dew point temperature and relative humidity values at the airports with and without precipitation. In snowy times, lower temperature and higher relative humidity values were determined compared to the whole period. Also, the whole period temperature average at LTBA was about 0.9 °C during whole period (BS-Events and SYNOP-Events on average), while it was 0.2 °C during snowy times. Therefore, one of the biggest reasons why snow was not observed at LTBA in the presence of BS-Events and SYNOP-Events was the course of surface temperatures around 0.9 °C.

Table 6 Wind direction variation between 1000 hPa and upper atmospheric levels

	Wind Shear (1000–850 hPa)	Wind Shear (1000–700 hPa)
BS	35°	40°
OSC	60°	80°
SYNOP	40°	35°
TRANS	30°	45°

Acknowledgements This work is funded by the Turkish Science Foundation (TUBITAK) with Grant Number 1059B142000051. The authors would like to thank the Turkish State Meteorological Service for the data used in this study. The authors also thank the Writing Center of the University of Missouri for their assistance.

Author contribution Veli Yavuz: conceptualization, methodology, formal analysis, writing—original draft. Anthony R. Lupo: conceptualization, formal analysis, supervision, writing—eview and editing.
Neil I. Fox: supervision, writing—review and editing.
Ali Deniz: supervision, writing—review and editing.

Funding Work is funded by the Turkish Science Foundation (TUBITAK) with Grant Number 1059B142000051.

Data availability Not applicable.

Declarations

Ehtics approval Not applicable.

Patient consent Not applicable.

Clinical trial registration Not applicable.

Permission to reproduce material from other sources Not applicable.

Conflict of interest The authors declare no conflict of interest.

References

Alcott TI, Steenburgh WJ, Laird NF (2012) Great Salt Lake effect precipitation: observed frequency, characteristics, and associated environmental factors. Weather Forecast 27:954–971. https://doi.org/10.1175/WAF-D-12-00016.1

APDRC (2021) Asia-Pacific Data-Research Center: sea surface temperatures. http://apdrc.soest.hawaii.edu. Accessed 10 September 2021

Ballentine RJ (1992) Numerical simulation of land-breeze-induced snow bands along the western shore of Lake Michigan. Mon Wea Rev 110(11):1544–1553. https://doi.org/10.1175/1520-0493(1982)110%3c1544:NSOLBI%3e2.0.CO;2

Baltaci H, da Silva MCL, Gomes HB (2021) Climatological conditions of the Black Sea-effect snowfall events in Istanbul. Turkey Int J Climatol 41(3):2017–2028. https://doi.org/10.1002/joc.6944

Braham RR Jr (1983) The Midwest snowstorm of 8–11 December 1977. Mon Wea Rev 111(2):253–272. https://doi.org/10.1175/1520-0493(1983)111%3c0253:TMSSOD%3e2.0.CO;2

Demirarslan KO, Akinci H (2018) Assessment of Winter Season Air Quality in the Marmara Region Using GIS and Air Quality Data. J Nat Hazards Environ 4(1):11–27 (in Turkish)

Ellis AW, Leathers DJ (1996) A synoptic climatological approach to the analysis of lake-effect snowfall: potential forecasting applications. Weather Forecast 11(2):216–229. https://doi.org/10.1175/1520-0434(1996)011%3c0216:ASCATT%3e2.0.CO;2

Forbes GS, Merritt JH (1984) Mesoscale vortices over the Great Lakes in wintertime. Mon Wea Rev 112:377–381. https://doi.org/10.1175/15200493(1984)112%3C0377:MVOTGL%3E2.0.CO;2

Hartnett JJ, Collins JM, Baxter MA, Chambers DP (2014) Spatiotemporal snowfall trends in Central New York. J Appl Meteorol Climatol 53(12):2685–2697. https://doi.org/10.1175/JAMC-D-14-0084.1

Holroyd EW III (1971) Lake-effect cloud bands as seen from weather satellites. J Atmos Sci 28(7):1165–1170. https://doi.org/10.1175/1520-0469(1971)028%3c1165:LECBAS%3e2.0.CO;2

IOWA (2021) Environmental Mesonet: ASOS-AWOS-METAR data. https://mesonet.agron.iastate.edu/request/download.phtml. Accessed 8 September 2021

Kelly RD (1982) A single doppler radar study of horizontal-roll convection in a lake-effect snow storm. J Atmos Sci 39(7):1521–1531. https://doi.org/10.1175/1520-0469(1982)039%3c1521:ASDRSO%3e2.0.CO;2

Kelly RD (1986) Mesoscale frequencies and seasonal snowfalls for different types of Lake Michigan snow storms. J Atmos Appl Meteorol 25:308–312. https://doi.org/10.1175/1520-0450(1986)025%3c0308:MFASSF%3e2.0.CO;2

Kindap T (2010) A severe sea-effect snow episode over the city of Istanbul. Nat Hazards 54:707–723. https://doi.org/10.1007/s11069-009-9496-7

Kristovich DAR, Laird NF (1998) Observations of widespread lake-effect cloudiness: Influences of upwind conditions and lake surface temperatures. Weather Forecast 13(3):811–821. https://doi.org/10.1175/1520-0434(1998)013%3c0811:OOWLEC%3e2.0.CO;2

Kristovich DAR, Laird NF, Hjelmfelt MR (2003) Convective evolution across Lake Michigan during a widespread lake-effect snow event. Mon Wea Rev 131(4):643–655. https://doi.org/10.1175/1520-0493(2003)131%3c0643:CEALMD%3e2.0.CO;2

Laird NF, Kristovich DAR (2004) Comparison of observations with idealized model results for a method to resolve winter lake-effect mesoscale morphology. Mon Wea Rev 132:1093–1103. https://doi.org/10.1175/1520-0493(2004)132%3c1093:COOWIM%3e2.0.CO;2

Laird NF, Desrochers J, Payer M (2009a) Climatology of lake-effect precipitation events over Lake Champlain. J Appl Meteorol 48(2):232–250. https://doi.org/10.1175/2008JAMC1923.1

Laird NF, Sobash R, Hodas N (2009b) The frequency and characteristics of lake-effect precipitation events associated with the New York State Finger Lakes. J Appl Meteorol Climatol 48(4):873–886. https://doi.org/10.1175/2008JAMC2054.1

Laird NF, Bentley AM, Ganetis SA, Stieneke A, Tushaus SA (2016) Climatology of lake-effect precipitation events over Lake Tahoe and Pyramid Lake. J Appl Meteorol Climatol 55(2):297–312. https://doi.org/10.1175/JAMC-D-14-0230.1

Lazri M, Labadi K, Brucker JM, Ameur S (2020) Improving satellite rainfall estimation from MSG data in Northern Algeria by using a multi-classifier model based on machine learning. J Hydrol 584:1–16. https://doi.org/10.1016/j.jhydrol.2020.124705

Metz ND, Bruick ZS, Capute PK, Neureuter MM, Ott EW, Sessa MF (2019) An investigation of cold-season short-wave troughs in the great lakes region and their concurrence with lake-effect clouds. J Appl Meteorol Climatol 58(3):605–614. https://doi.org/10.1175/JAMC-D-18-0177.1

Miner TJ, Fritsch JM (1997) Lake-Effect Rain Events. Mon Wea Rev 125(12):3231–3248. https://doi.org/10.1175/1520-0493(1997)125%3c3231:LERE%3e2.0.CO;2

NASA (2021) National Aeronautics and Atmospheric Administration. http://lance-modis.eosdis.nasa.gov/cgi-bin/imagery/realtime.cgi?date=2009058. Accessed 11 September 2021

Niziol TA (1987) Operational forecasting of lake effect snowfall in western and central New York. Weather Forecast 2(4):310–321. https://doi.org/10.1175/1520-0434(1987)002%3c0310:OFOLES%3e2.0.CO;2

Niziol TA, Snyder WR, Waldstreicher JS (1995) Winter weather forecasting throughout the eastern United States. Part IV: lake effect snow. Weather Forecast 10(1):61–77. https://doi.org/10.1175/1520-0434(1995)010%3c0061:WWFTTE%3e2.0.CO;2

Passarelli RE Jr, Braham RR Jr (1981) The role of the winter land breeze in the formation of Great Lakes snow storms. Bull Amer Meteor Soc 62(4):482–491. https://doi.org/10.1175/1520-0477(1981)062%3c0482:TROTWL%3e2.0.CO;2

Pike WS, Webb JDC (2020) The very deep cold pool, and lake-effect snowfalls of 27 February–1 March 2018. Weather 75(3):88–98. https://doi.org/10.1002/wea.3675

PSWC (2021) Plymouth State Weather Center: Upper air charts. https://vortex.plymouth.edu/myo/upa. Accessed 8 September 2021

Reinking RF, Caiazza R, Kropfli RA, Orr BW, Martner BE, Niziol TA, Byrd GP, Penc RS, Zamora RJ, Snider JB, Ballentine RJ, Stamm AJ, Bedford CD, Joe P, Koscielny AJ (1993) The Lake Ontario Winter Storms (LOWS) project. Bull Am Meteor Soc 74:1828–1849

Rothrock HJ (1969) An aid in forecasting significant lake snows. Tech. Memo. WBTM CR-30, National Weather Service, Central Region, Kansas City, MO, p 12

Scott CPJ, Sousounis PJ (2001) The utility of additional soundings for forecasting lake-effect snow in the Great Lakes Region. Weather Forecast 16(4):448–462. https://doi.org/10.1175/1520-0434(2001)016%3c0448:TUOASF%3e2.0.CO;2

Smith BB, Boris JP (2017) Lake snow parameter. National Weather Service Forecast Office, Gaylord, MI. https://www.weather.gov/apx/lake_snow_parameter. Accessed 5 September 2021

Steenburgh WJ, Halvorson SF, Onton DJ (2000) Climatology of lake-effect snowstorms of the Great Salt Lake. Mon Wea Rev 128:709–727. https://doi.org/10.1175/1520-0493(2000)128%3c0709:COLESO%3e2.0.CO;2

Suriano ZJ, Leathers DJ (2017) Synoptically classified lake-effect snowfall trends to the lee of Lakes Erie and Ontario. Clim Res 74:1–13. https://doi.org/10.3354/cr01480

Trigo IF, Dacamara CC, Viterbo P, Roujean JL, Olesen F, Barroso C, Camacho F, de Coca D, Freitas CSC, Garcia-Haro J, Geiger B, Gellens-Meulenberghs F, Ghilain N, Melia J, Pessenha L, Siljamo N, Arboleda A (2011) The satellite application facility for land surface analysis. Int J Remote Sens 32:2725–2744. https://doi.org/10.1080/01431161003743199

Tuttle JD, Davis CA (2013) Modulation of the diurnal cycle of warm-season precipitation by short-wave troughs. J Atmos Sci 70:1710–1726. https://doi.org/10.1175/JAS-D-12-0181.1

TSMS (2021) Turkish State Meteorological Service. http://www.mgm.gov.tr. Accessed 8 Sept 2021

University of Wyoming (2021) http://weather.uwyo.edu/upperair/sounding.html. Accessed 9 Sept 2021

Villani JP, Jurewicz ML, Reinhold K Sr (2017) Forecasting the Inland Extent of Lake Effect Snow Bands Downwind of Lake Ontario. J Oper Meteorol 5(5):53–70. https://doi.org/10.15191/nwajom.2017.0505

Wiley J, Mercer A (2020) An updated synoptic climatology of Lake Erie and Lake Ontario heavy lake-effect snow events. Atmosphere 11(8):872. https://doi.org/10.3390/atmos11080872

Yavuz V, Deniz A, Özdemir ET (2021a) Analysis of a vortex causing sea-effect snowfall in the western part of the Black Sea: a case study of events that occurred on 30–31 January 2012. Nat Hazards 108:819–846. https://doi.org/10.1007/s11069-021-04707-8

Yavuz V, Deniz A, Özdemir ET, Kolay O, Karan H (2021b) Classification and analysis of sea-effect snowbands for Danube Sea are in Black Sea. Int J Climatol 41(5):3139–3152. https://doi.org/10.1002/joc.7010

Yavuz V, Lupo AR, Fox NI, Deniz A (2022a) Meso-scale comparison of non-sea-effect and sea-effect snowfalls, and development of prediction algorithm for megacity Istanbul airports in Turkey. Atmosphere 13(5):657. https://doi.org/10.3390/atmos13050657

Yavuz V, Lupo AR, Fox NI, Deniz A (2022b) The role of short-wave troughs on the formation and development of sea-effect snowbands in the western Black Sea. Nat Hazards. https://doi.org/10.1007/s00704-022-04071-y

Zhao W, Duan SB (2020) Reconstruction of daytime land surface temperatures under cloud-covered conditions using integrated MODIS/Terra land products and MSG geostationary satellite data. Remote Sens Environ 247:1–15. https://doi.org/10.1016/j.rse.2020.111931